Available online at www.sciencedirect.com
ScienceDirect
Journal of Hazardous Materials 158 (2008) 88–99
Journal of Hazardous Materials
www.elsevier.com/locate/jhazmat

On pool spreading around tanks: Geometrical considerations

Sara Brambilla, Davide Manca *

Politecnico di Milano, Dipartimento di Chimica, Materiali e Ingegneria Chimica "Giulio Natta", Piazza Leonardo da Vinci 32, 20133 Milano, Italy

Received 12 December 2007; received in revised form 10 January 2008; accepted 11 January 2008
Available online 20 January 2008

Abstract

The paper discusses a straightforward approach for evaluating the distance covered by a spreading liquid pool, when the axisymmetric hypothesis is no longer valid. This distance is evaluated by a three-steps methodology: the pre-processing of input data (bund radius, if present, and radial velocity); the simulation of pool spreading by a model based on the axisymmetric hypothesis; and the post-processing of results. The paper reports some geometrical correlations to pre- and post-process the data, with regard to four case-studies. Some numerical examples are also presented to prove that the pre-processed input data and post-processed results differ from those based on the axisymmetric hypothesis. Finally, we validate our modeling approach with the experimental data of Cronin and Evans [P.S. Cronin, J.A. Evans, A series of experiments to study the spreading of liquid pools with different bund arrangements, HSE Contract Research Report 405/2002, Advantica Technologies Limited, 2002].

Keywords: Pool spreading; Pool shape; Industrial accident; Emergency planning; Pre-processing; Post-processing

1. Problem statement

The modeling of chemical accidents involves the determination of the potential accident outcomes and their impact on people, facilities, properties, communication networks, and so forth. Both emergency preparedness and response activities are involved in the modeling of accidents to determine the distance at which certain dangerous thresholds are exceeded (the toxic threshold in case of gas releases; the radiative heat flux for fires; the overpressure for explosions). By doing so, the emergency preparedness can significantly improve the mitigation of adverse consequences as well as the emergency planning. Conversely, under emergency response, such information may help identifying the proper actions (alarms, evacuation procedures, workers rescue, etc.).

This paper deals with the accident modeling, by re-examining a well-known phenomenon from a new perspective. In particular, the attention is focused on accidents involving the spillage of a liquid onto a surface (i.e., liquid pools). We will try to answer the question: which shape will the liquid pool take?

The literature models for risk assessment (e.g. [1–7]) characterize the pool evolution in terms of pool radius, height, volume, and temperature. They consider also the discharge rate of liquid into the pool and the evaporation rate from the pool. When working in the field of risk assessment, it is mandatory to model both the pool radius and the evaporation rate. The evaporation rate and the pool area allow evaluating the vapor emitted to the atmosphere and then dispersed. On the other hand, the pool radius corresponds to the extent of liquid pool that influences the area involved in the accident and, consequently, the arrangement of the mitigation system as well as the emergency planning. Therefore, when a liquid spreads onto a surface, the estimation of the pool radius is an important step in risk assessment.

Usually, literature models consider a punctiform release that is perfectly perpendicular to the surface. In other words, these models evaluate the pool dynamics according to the axisymmetric hypothesis, i.e., the pool spreads in all directions at the same velocity. Consequently, the spreading pool has a circular shape under the axisymmetric hypothesis.

However, we will determine some geometrical correlations to remove this restrictive hypothesis. In fact, when a liquid is poured onto a surface, it can spread in several directions with a different velocity, and consequently it assumes a different shape, which depends on the pouring conditions. The circular pool is only an abstraction that makes simpler the modeling of the pool spreading, but, under real conditions, it probably never occurs. Nonetheless, literature models assume the axisymmetric spreading [1,4–6].

* Corresponding author. Tel.: +39 02 23993271; fax: +39 02 70638173.
E-mail address: davide.manca@polimi.it (D. Manca).

0304-3894/$ – see front matter © 2008 Elsevier B.V. All rights reserved.
doi:10.1016/j.jhazmat.2008.01.049

Nomenclature

A	area (m^2)
A, B	intersection points
r	radius (m)
u	radial velocity (m/s)
x, y	reference frame coordinates

Greek letters

α, θ	angles (rad)

Subscripts

axi	axisymmetric case
B	bund
e	corrected value
P	pool

Let us now consider the following trivial examples. If one pours some water (from a bottle onto a table) perfectly perpendicular to the surface, the water will spread in all directions at the same velocity (axisymmetric spreading), giving rise to a circular pool. On the other hand, if one knocks over a glass of water, the pool will take a shape that is more similar to a long and narrow ellipse than to a circle.

An example closer to the chemical industry is a liquid spill from a hole in a process unit (a reactor, a tank, a pipe, etc.). Let us assume that there is a hole in a tank. The tank itself and the neighboring equipment will affect the pool shape, since the spreading liquid may reach the tank wall and assume neither a circular shape nor an elliptical one. In addition, the impact angle between the surface and the liquid jet will influence the pool shape. If the liquid jet is not perpendicular to the surface, the pool will take an elongated shape in the direction of the jet, due to the leading velocity in that direction.

This paper proposes some geometrical correlations to determine the pool extent, depending on the accidental circumstances. We do not develop a new model, because it is not a trivial activity and we should develop *ad hoc* models for each specific situation, losing both the generality and the wide applicability of results. Instead, we suggest some geometrical formulae to convert the input and output data of the available literature models that assume an axisymmetric spreading, because these models are consolidated, well accepted, and validated. By doing so, the results we bring forth can be used to model the pool spreading and/or shrinking by means of a literature model based on the axisymmetric hypothesis. Afterward, the output results can be post-processed to adapt them to the relative pool-tank arrangement.

We are proposing some geometrical correlations that should be implemented to pre-process the input data as well as to post-process the output results of the spreading simulator.

As far as the input data are concerned, the variables that must be pre-processed, in order to translate the real world conditions to the ideal representation, according to the axisymmetric hypothesis, are the bund radius (if present) and the radial velocity. The radial velocity is the edge velocity of the pool, i.e., the spreading rate. If the liquid is discharged with a null component of the velocity parallel to the surface, then the radial velocity is influenced only by the pool height (liquid head) and by the friction between the pool and the underlying surface. Conversely, the discharge velocity influences the pool radial velocity. In the former case, the liquid hits the ground perfectly perpendicular, whilst in the latter, the liquid jet is inclined respect to the vertical and there is a component of the velocity parallel to the surface. Therefore, the radial velocity must be pre-processed because it affects the spreading rate and the pool extension.

With reference to the output data, the pool radius is the variable that must be post-processed. Actually, we make use of the results from a model based on the axisymmetric spreading hypothesis to evaluate what happens in the real world.

We developed the aforementioned geometrical correlations to provide a more realistic picture of the liquid pool and its distance from the process units. These correlations where intended to transform the output results of real-time accident simulation programs. This kind of accident simulators is particularly suited for the emergency response as well as operator training. Obviously, computational fluid dynamics (CFD) programs are not suitable for these objectives. CFD programs might enhance the realism, but they are still too time-consuming.

In the following sections, we will discuss some case-studies concerning the radial spreading of a liquid around a cylindrical tank, and the spreading of a pool spilled from a hole in both a parallelepiped and cylindrical tank. Finally, to validate the proposed correlations, we compare our numerical simulations with a set of experimental data [8].

2. Case-studies

This section discusses four case-studies, representative of the problem under consideration. Further alternatives can be added by modifying the environment surrounding the pool or the leakage conditions.

For each case-study, we describe how to re-evaluate the bund radius, the radial velocity (input data) and the pool radius (output data). Case-study 1 introduces the axisymmetric hypothesis (reference case); case-study 2 discusses the radial spreading of a liquid around a cylindrical tank; while case-studies 3 and 4 analyze the spreading of a pool spilled from a hole, respectively, in a parallelepiped and in a cylindrical tank. For each case-study, we work with a conventional literature model that simulates the simplified and ideal axisymmetric spreading but we also need to translate the required input data and the output simulated results to get a correct interpretation of what effectively happens in the real world.

All the figures, reported in the following, are top views of the proposed case-studies. In addiction, the liquid will be cyan, the tank bright-gray, and the bund dark-gray.

2.1. Case-study 1: the axisymmetric pool

The axisymmetric, circular pool, represented in Fig. 1, is the reference case. By assuming that the pool radius is r_P, the pool area can be evaluated as: $A_{P,axi} = \pi r_P^2$.

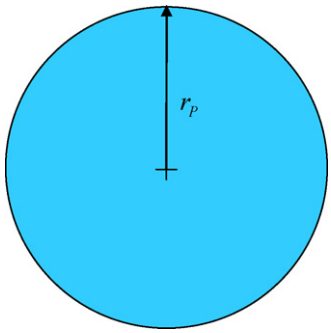

Fig. 1. Reference case—the axisymmetric pool.

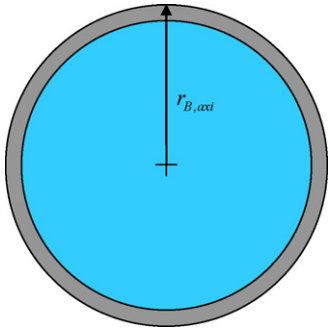

Fig. 2. Reference case—bund representation.

If a bund is present (i.e., the dark-gray corona of Fig. 2) its internal radius is $r_{B,axi}$, and the pool will not spread over it. In that case, the area confined within the bund is: $A_{B,axi} = \pi r_{B,axi}^2$.

The reference case identifies the pool radial velocity as u.

2.2. Case-study 2: radial spreading around a cylindrical tank

If a uniform liquid leakage occurs around the whole perimeter of the tank, the spreading pool will assume a corona geometry, as represented in Fig. 3 (cyan in web version), where the tank takes up the internal portion (bright-gray). In this condition, the pool radius is defined as the "corrected radius" and assumes the following symbology: r_e.

First, we want to evaluate the corrected radius r_e from the output results of a model based on the axisymmetric spreading hypothesis that evaluates the conventional pool radius r_P as a function of time. We suggest to determine the corrected radius, r_e, by assuming that the pool volume is the same both in this case and in the reference one. Also, we assume that the pool height is practically the same independently of the spreading hypothesis, i.e., either for the circular pool or the corona one. Consequently, we propose the conservation of pool areas between the ideal and real models.

For the corona geometry, the pool area is

$$A_P = \pi(r_e^2 - r_T^2)$$

Then, by making it equal it to the pool area of the reference case:

$$A_{P,axi} = A_P \Rightarrow \pi r_P^2 = \pi(r_e^2 - r_T^2)$$

the corrected radius follows:

$$r_e = \sqrt{r_P^2 + r_T^2} \quad (1)$$

The difference between r_e and r_P increases with the tank radius.

If a circular bund of radius r_B surrounds the tank, as shown in Fig. 4, its radius must be pre-processed to perform a simulation with a model based on the axisymmetric hypothesis. By doing so, even for the axisymmetric simulation, the pool does not spread indefinitely, but its extent is limited.

If we assume that the bund of the reference case encloses the same area as the current bund, then

$$A_{B,axi} = A_B \Rightarrow \pi r_{B,axi}^2 = \pi(r_B^2 - r_T^2)$$

Therefore, with reference to the model based on the axisymmetric hypothesis, the bund radius ($r_{B,axi}$) is:

$$r_{B,axi} = \sqrt{r_B^2 - r_T^2} \quad (2)$$

The difference between $r_{B,axi}$ and r_B increases with the tank radius.

If a bund is present, Eq. (1) is valid as long as $r_e < r_B$.

If the pool has a radial velocity u_e, it can be translated into a value useful for the axisymmetric model by assuming that

$$u_e = \frac{dr_e}{dt}$$

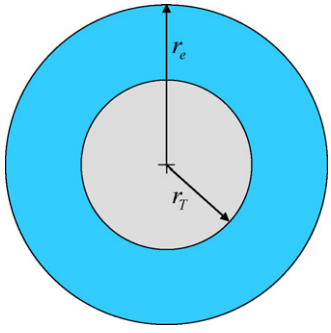

Fig. 3. Radial spreading around a cylindrical tank.

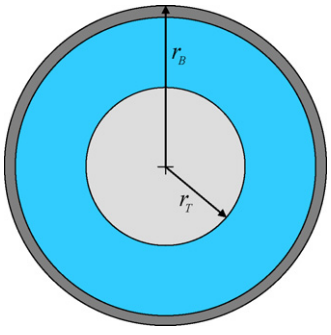

Fig. 4. Radial spreading of a pool around a cylindrical tank, when a bund is present.

and by substituting Eq. (1):

$$\frac{dr_e}{dt} = \frac{r_P}{\sqrt{r_P^2 + r_T^2}} \frac{dr_P}{dt}$$

Recalling that

$$\frac{dr_P}{dt} = u$$

it is possible to derive

$$u = u_e \frac{\sqrt{r_P^2 + r_T^2}}{r_P} \quad (3)$$

The difference between u_e and u increases with the tank radius.

2.3. Case-study 3: pool spreading from a hole in a parallelepiped tank

When a hole forms in a process unit full of liquid, the liquid spills and a pool spreads in front of it. In this case, we assume that the apparatus is a parallelepiped tank and the pool takes up a semicircular shape in front of it (see Fig. 5).

Again, by assuming the pool area conservation hypothesis:

$$A_{P,axi} = A_P \Rightarrow \pi r_P^2 = \frac{\pi r_e^2}{2}$$

the corrected pool radius becomes

$$r_e = \sqrt{2} r_P \quad (4)$$

The tank dimension does not affect the corrected radius.

If a bund at a distance r_B from the tank wall is present, for the configuration showed in Fig. 6, we consider two consecutive phases. The first phase finishes when the pool reaches the bund and the corrected radius is evaluated according to Eq. (4).

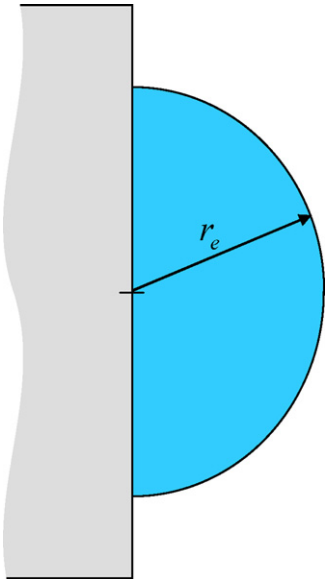

Fig. 5. Semicircular pool in front of a parallelepiped tank.

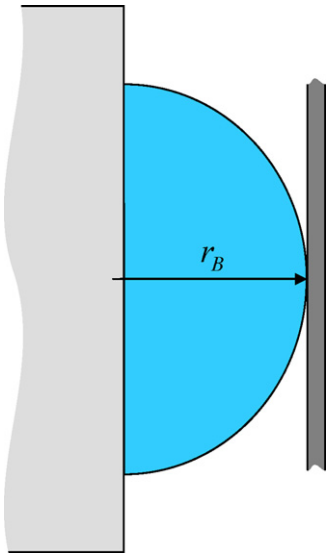

Fig. 6. Semicircular bund in front of a parallelepiped tank.

When the pool reaches the bund, it changes its shape and starts spreading laterally, up to completely filling the bund. Furthermore, the contact of pool with the bund can generate a reflected wave. Therefore, the hypothesis on pool area conservation could not be valid to simulate the situation shown in Fig. 7.

As aforementioned, this is a rather simplified analysis, so the determination of any geometrical correlations to describe the evolution of the pool, until the bund filling, is beyond the purpose of this paper. Therefore, our modeling approach cannot characterize the whole pool behavior up to the bund filling, but it gives an idea of the phenomenon, even if only for a limited period (as long as $r_e < r_B$).

We choose to evaluate the bund radius for the axisymmetric simulation from the total area of the real bund:

$$A_{B,axi} = \pi r_{B,axi}^2 = A_B \quad (5)$$

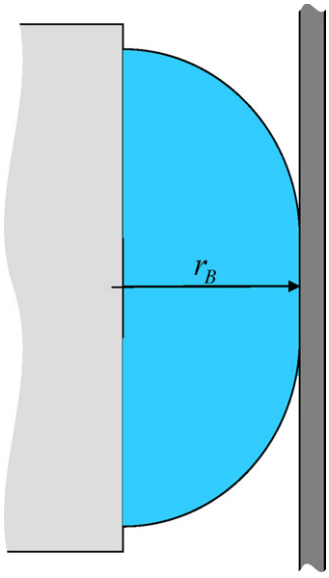

Fig. 7. Pool elongated laterally.

If the pool has a radial velocity u_e, before the pool reaches the bund, it can be translated into a corresponding value for the axisymmetric model by assuming that

$$u_e = \frac{dr_e}{dt} = \sqrt{2}\frac{dr_P}{dt} = \sqrt{2}u$$

which means

$$u = \frac{u_e}{\sqrt{2}} \tag{6}$$

2.4. Case-study 4: pool spreading from a hole in a cylindrical tank

As in the previous case, in this section we are considering the formation of a pool in front of a tank, but here, the tank is cylindrical. In this case, we assume that the leakage forms a semicircle pool in front of the tank, as shown in Fig. 8. In the real situations, the pool boundary will not be so sharp, but this simplification allows performing an easier analysis. In the following, we discuss also a more detailed analysis.

By applying, once again, the pool area conservation hypothesis:

$$A_{P,axi} = A_P \Rightarrow \pi r_P^2 = \frac{\pi}{2} r_e^2$$

the corrected radius is

$$r_e = \sqrt{2} r_P \tag{7}$$

In this case, the tank dimension does not affect the corrected radius.

If a bund is present, as in the configuration of Fig. 9, the previous analysis, i.e., Eq. (7), is valid till the pool reaches the bund: $r_e = r_B - r_T$.

After that, the pool starts spreading laterally, as sketched in Fig. 10 and a reflected wave may form.

As in the previous case, this approach cannot completely describe the liquid behavior, but it gives an idea of the phenomenon, even if only for a limited period ($r_e < r_B - r_T$).

The bund radius for the axisymmetric case can be evaluated by considering that the bund contains the same volume of liquid

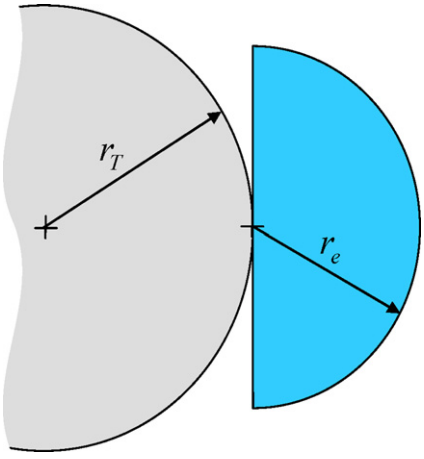

Fig. 8. Semicircular pool in front of a cylindrical tank: simplified representation.

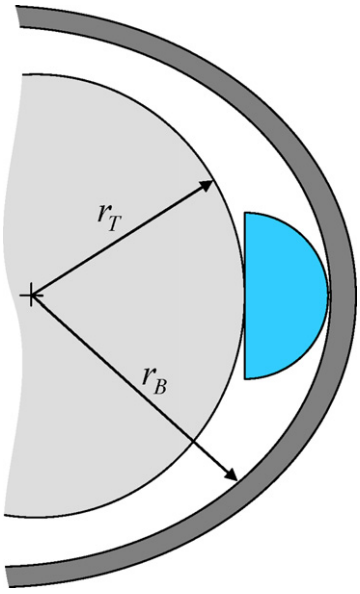

Fig. 9. Semicircular bund in front of a cylindrical tank: simplified representation.

(and consequently the same pool area):

$$A_{B,axi} = A_B \Rightarrow \pi r_{B,axi}^2 = \pi(r_B^2 - r_T^2)$$

hence

$$r_{B,axi} = \sqrt{r_B^2 - r_T^2} \tag{8}$$

The difference between $r_{B,axi}$ and r_B increases with the tank radius.

If the pool has a radial velocity u_e, it can be translated into a useful value for the axisymmetric model by assuming that

$$u_e = \frac{dr_e}{dt} = \sqrt{2}\frac{dr_P}{dt} = \sqrt{2}u$$

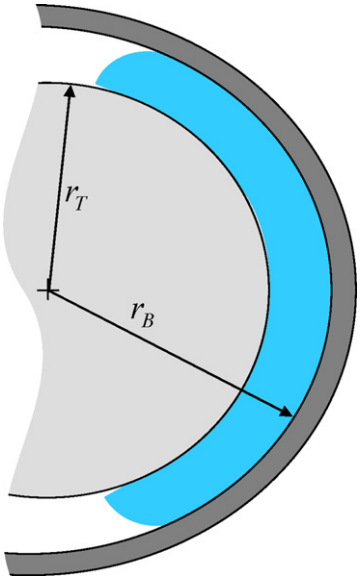

Fig. 10. Lateral spreading of the pool.

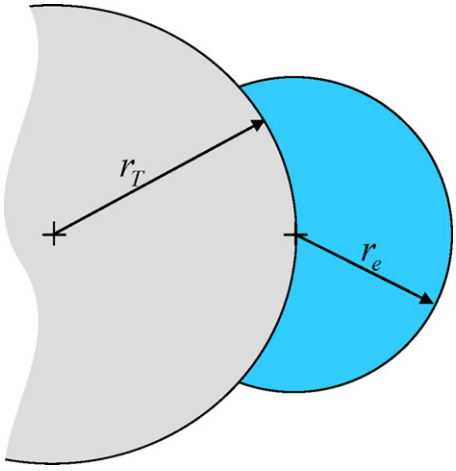

Fig. 11. Semicircular pool in front of a cylindrical tank: a more realistic representation.

which means

$$u = \frac{u_e}{\sqrt{2}} \tag{9}$$

A more realistic representation will lead to the condition sketched in Fig. 11, where the pool surrounds the tank, due also to the surface tension among the liquid, the ground, and the tank skin.

In this case, the procedure for deriving the corrected radius r_e is not explicit but numerical: it requires the solution of a nonlinear algebraic equation. The tank and the pool are represented like two circumferences on the same axis (see Fig. 12), which intersect at points A and B.

The first step requires determining the equations of the two circumferences. We assume that the center of the circumference representing the tank is the center of the x–y-axes, while the center of the pool is at the tank wall on the x-axis. It follows:

$$x^2 + y^2 - r_T^2 = 0 \quad \text{for the tank}$$

$$x^2 + y^2 - 2r_T x + r_T^2 - r_e^2 = 0 \quad \text{for the pool}$$

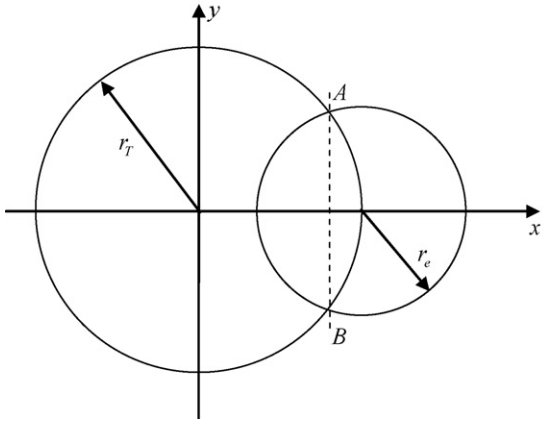

Fig. 12. Geometrical schematization of the problem.

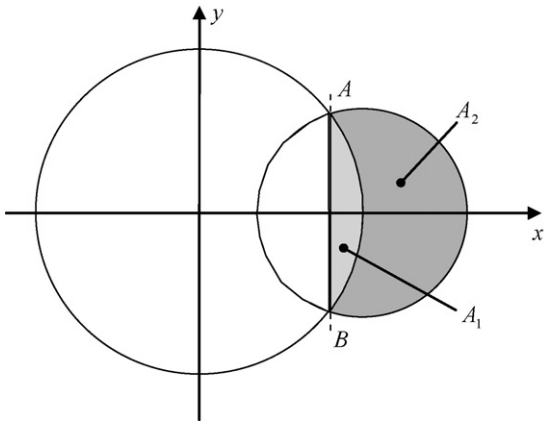

Fig. 13. Area identification.

The following step involves the analytical determination of the coordinates of points A and B:

$$A \equiv \left(\frac{2r_T^2 - r_e^2}{2r_T}; +r_e \sqrt{1 - \frac{r_e^2}{4r_T^2}} \right),$$

$$B \equiv \left(\frac{2r_T^2 - r_e^2}{2r_T}; -r_e \sqrt{1 - \frac{r_e^2}{4r_T^2}} \right)$$

The effective pool area is the dark-gray portion of the smaller circumference of Fig. 13.

The integral calculus allows determining this area. The effective pool area (A_2) can be evaluated as the difference between the dark-gray plus the bright-gray areas ($A_1 + A_2$) and the bright-gray area (A_1). Such a difference can be evaluated by means of two definite integrals (see Appendix A for more details).

By assuming that θ is the angle between the x-axis and the line between the center of the tank circumference and the intersection point A (see Fig. 20), the bright-gray is

$$A_1 = \int_{x_A}^{r_T} \sqrt{r_T^2 - x^2}\, dx = r_T^2(\theta - \sin\theta\cos\theta) \tag{10}$$

By assuming that α is the angle between the x-axis and the line between the pool center and the intersection point A (see Fig. 20), the area of the dark-gray plus the bright-gray portion is

$$A_1 + A_2 = \int_{x_A}^{r_P} \sqrt{2r_T x - r_T^2 + r_e^2 - x^2}\, dx$$
$$= r_e^2(\alpha - \sin\alpha\cos\alpha) \tag{11}$$

Finally, the dark-gray area is

$$A_2 = (A_1 + A_2) - A_1 = r_e^2(\alpha - \sin\alpha\cos\alpha) - r_T^2(\theta - \sin\theta\cos\theta) \tag{12}$$

To determine the corrected radius, r_e, this area must be equal to the area of the reference case (i.e., the axisymmetric pool

$A_{P,axi} = \pi r_P^2$), that is:

$$\pi r_P^2 = r_e^2(\alpha - \sin\alpha\cos\alpha) - r_T^2(\theta - \sin\theta\cos\theta) \quad (13)$$

The trigonometric relations referred to the intersection points allow determining the angles α and θ:

$$x_A = \frac{2r_T^2 - r_e^2}{2r_T} = r_T\cos\theta = r_T + r_e\cos\alpha,$$

$$y_A = r_e\sqrt{1 - \frac{r_e^2}{4r_T^2}} = r_T\sin\theta = r_e\sin\alpha$$

This means that it is not possible to find an explicit solution because the corrected radius, r_e, is present in both the expressions of α and θ. Therefore, we have to solve numerically Eq. (13) to find r_e. This analysis is correct up to $r_e \le 2r_T$, because for $r_e > 2r_T$ there are no more intersection points between the two circumferences.

If we adopt the bisection method for the root-finding, we need two extremes of an interval $[a, b]$ where the function changes sign. In this case, the two extremes are zero and twice the tank radius. As far as the Newton method is concerned, a possible first guess point is the value of the axisymmetric pool radius.

Fig. 14 sketches the condition when a bund is present. The bund radius for the axisymmetric case can be evaluated as

$$A_{B,axi} = A_B \Rightarrow \pi r_{B,axi}^2 = \pi(r_B^2 - r_T^2)$$

then

$$r_{B,axi} = \sqrt{r_B^2 - r_T^2} \quad (14)$$

As in the previous case, when the pool reaches the bund, it starts spreading laterally and a reflected wave may form. Therefore, the solution of Eq. (13) allows evaluating the pool radius when $r_e \le r_B - r_T$.

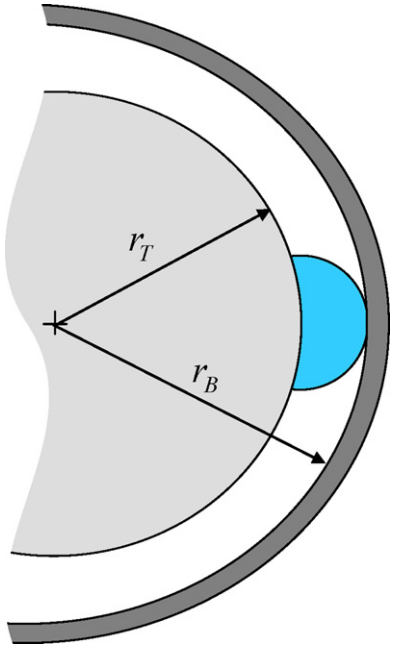

Fig. 14. Semicircular pool in front of a cylindrical tank: presence of the bund.

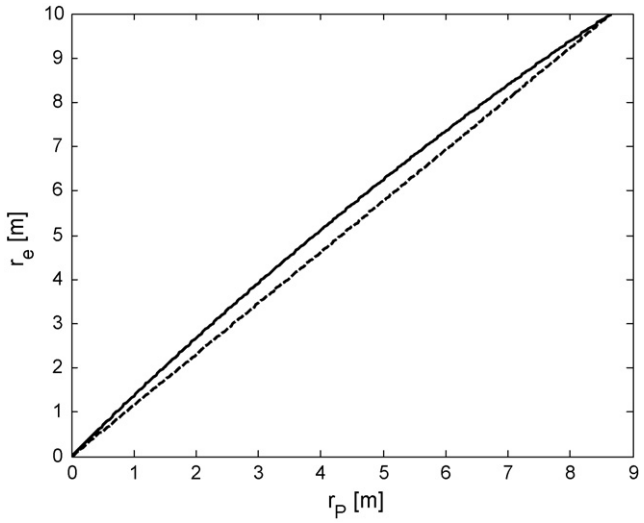

Fig. 15. The corrected radius as a function of the pool axisymmetric radius, assuming a tank radius of 5 m (solid line). The dashed line is a linear approximation of the solid line.

By assuming the same notation of Fig. 10, the total extent of the pool is

$$2(r_B - r_T) + r_{L2} \quad (15)$$

The conversion of the radial velocity from u_e to u calls for determining the relation between r_e and r_P, and eventually the relation between dr_e/dt and dr_P/dt. Since the relation between r_e and r_P is not explicit, we cannot determine an explicit relation between u_e and u. Consequently, we will try to approximate the relation between u_e and u.

Fig. 15 sketches the corrected radius versus the pool radius, for a cylindrical tank of 5 m radius. The maximum corrected radius is twice the tank radius, i.e., 10 m in this case. As a matter of fact, the diagram would have the same trend for both small and big tanks. The relation between r_e and r_P is almost linear. Thus, for our purpose, a straight line (dashed line of Fig. 15) well approximates such a relation. It is then possible to assume the radial velocity for the axisymmetric simulation to be equal to the radial velocity of the real configuration:

$$u = u_e \quad (16)$$

2.5. Summary of the case-studies

Table 1 summarizes the formulae discussed in previous sections.

In this section, we suggested some geometrical correlations to evaluate the radii of the pool and the bund and the radial velocity in some configurations differing from the reference case that is based on the axisymmetric hypothesis. These correlations allow determining the distance covered by the liquid when it is spilled from a process unit. In the following section, we discuss the importance of the proposed modeling approach by showing the difference between the distance reached by the pool in the reference case and that covered in real conditions.

Table 1
Summary of formulae

Case (#)	Description	Corrected pool radius (m)	Bund radius for the axisymmetric case (m)	Radial velocity for the axisymmetric case (m/s)
2	Radial spreading around a cylindrical tank	$r_e = \sqrt{r_P^2 + r_T^2}$	$r_{B,axi} = \sqrt{r_B^2 - r_T^2}$	$u = u_e \frac{\sqrt{r_P^2+r_T^2}}{r_P}$
3	Pool spreading from a hole in a parallelepiped tank	$r_e = \sqrt{2} r_P$	$r_{B,axi} = \sqrt{\frac{A_B}{\pi}}$	$u = \frac{u_e}{\sqrt{2}}$
4a	Pool spreading from a hole in a cylindrical tank (simplified case)	$r_e = \sqrt{2} r_P$	$r_{B,axi} = \sqrt{r_B^2 - r_T^2}$	$u = \frac{u_e}{\sqrt{2}}$
4b	Pool spreading from a hole in a cylindrical tank (more rigorous case)	Numerical procedure	$r_{B,axi} = \sqrt{r_B^2 - r_T^2}$	$u = u_e$

3. Numerical examples

The input data of this section are related to the previously described case studies, i.e., the bund radius, and the pool radial velocity. First, we pre-process the input data that are required by any simulation models based on the axisymmetric hypothesis. Then, we simulate the pool spreading. Eventually, we post-process the maximum distance reached by the axisymmetric pool to determine the corrected values of the real pool dimensions.

3.1. Pre-processing of data

We assume a cylindrical tank of 5 m radius, a bund of 10 m radius, and an initial radial velocity of 1.3 m/s.

According to the radial spreading model around a cylindrical tank (Section 2.2), the pool bund radius is

$$r_{B,axi} = \sqrt{r_B^2 - r_T^2} = \sqrt{(10)^2 - (5.0)^2} = 8.66\,\text{m}$$

and the radial velocity is

$$u = u_e \frac{\sqrt{r_P^2 + r_T^2}}{r_P} = 1.3 \frac{\sqrt{(2.3)^2 + (5.0)^2}}{2.3} = 3.11\,\text{m/s}$$

In case of pool spreading from a hole in a parallelepiped tank (Section 2.3), we assume that the tank and the bund have a square base, respectively, of 10 and 20 m. Hence, the total bund area is

$$A_B = r_B^2 - r_T^2 = 20^2 - 10^2 = 300\,\text{m}^2$$

and the bund radius is

$$r_{B,axi} = \sqrt{\frac{A_B}{\pi}} = \sqrt{\frac{300}{\pi}} = 9.77\,\text{m}$$

Finally, the radial velocity is

$$u = \frac{u_e}{\sqrt{2}} = \frac{1.3}{\sqrt{2}} = 0.92\,\text{m/s}$$

In case of pool spreading from a hole in a cylindrical tank (simplified case, Section 2.4), the bund radius is

$$r_{B,axi} = \sqrt{r_B^2 - r_T^2} = \sqrt{(10)^2 - (5.0)^2} = 8.66\,\text{m}$$

while the radial velocity is

$$u = \frac{u_e}{\sqrt{2}} = \frac{1.3}{\sqrt{2}} = 0.92\,\text{m/s}$$

In case of pool spreading from a hole in a cylindrical tank (detailed case, Section 2.4), the bund radius is again

$$r_{B,axi} = \sqrt{r_B^2 - r_T^2} = \sqrt{(10)^2 - (5.0)^2} = 8.66\,\text{m}$$

whereas the radial velocity is

$$u = u_e = 1.3\,\text{m/s}$$

Tables 2 and 3 summarize the pre-processed data, respectively, for the bund radius and the radial velocity, showing the differences among the reference case and the real configurations.

The differences between the bund radius, for the real configuration, and its axisymmetric value range from −14 to −2%. Conversely, the radial velocity differences range from −30 to +139%.

Table 2
Summary of the bund radii pre-processing

Case (#)	Description	Axisymmetric bund radius (m)	Difference from the reference case (m)
2	Radial spreading around a cylindrical tank	8.66	−1.34
3	Pool spreading from a hole in a parallelepiped tank	9.77	−0.23
4a	Pool spreading from a hole in a cylindrical tank (simplified case)	8.66	−1.34
4b	Pool spreading from a hole in a cylindrical tank (more rigorous case)	8.66	−1.34

Table 3
Summary of the pre-processing of radial velocity

Case (#)	Description	Radial velocity (m/s)	Difference from the reference case (m/s)
2	Radial spreading around a cylindrical tank	3.11	1.81
3	Pool spreading from a hole in a parallelepiped tank	0.92	−0.38
4a	Pool spreading from a hole in a cylindrical tank (simplified case)	0.92	−0.38
4b	Pool spreading from a hole in a cylindrical tank (more rigorous case)	1.3	0.00

We can conclude that the data pre-processing (for accident simulation) can lead to bund radii and radial velocities that differ significantly from the reference case based on the axisymmetric hypothesis.

3.2. Post-processing of data

Once the input data are pre-processed, it is possible to perform a simulation based on the axisymmetric hypothesis for each case-study. For the reference case, the pool reaches a maximum radius of 2.3 m and the maximum distance covered by the liquid is twice that value: 4.6 m.

With reference to a real case-study based on the radial spreading around a cylindrical tank (Section 2.2), the corrected pool radius is

$$r_e = \sqrt{r_P^2 + r_T^2} = \sqrt{(2.3)^2 + (5.0)^2} = 5.5\,\text{m}$$

In other words, the pool arrives at a distance of 0.5 m from the tank wall, which is quite smaller than the 4.6 m value determined by adopting the hypothesis of axisymmetric spreading.

In case of pool spreading from a hole in a parallelepiped tank (Section 2.3), the corrected pool radius (i.e., the distance covered by the pool) is

$$r_e = \sqrt{2} r_P = \sqrt{2}(2.3) = 3.25\,\text{m}$$

As in previous case, the distance reached by the pool is lower than that evaluated by the reference case.

In case of pool spreading from a hole in a cylindrical tank (simplified case, Section 2.4), the pool corrected radius is

$$r_e = \sqrt{2} r_P = \sqrt{2}(2.3) = 3.25\,\text{m}$$

This means that the pool will reach the distance of 3.25 m from the tank. As far as the more detailed representation is concerned, the numerical solution procedure determines a corrected radius of 3.06 m, which is a bit lower than the simplified case. Table 4 summarizes the simulated results, showing the differences among the reference case and the real configurations.

These examples show the importance of our corrected model. The literature models based on the axisymmetric hypothesis are too conservative. Actually, a systematic over-prediction of the maximum pool radius may be observed. We may observe relative errors between 30 and 90% respect to the standard literature models (based on the axisymmetric hypothesis). By adopting the pool area conservation hypothesis, the evaporation (which is a function of the pool area) will be the same for all cases, but, if a pool fire develops, the flames may envelope a lower number of process units. In addition, the heat radiative flux that impinges the neighboring process units may be significantly different due to the relative distance between the pool and the equipment as well as the pool shape and correlated view factors. Consequently, the mitigation systems (bunds, sprinklers, etc.) may be over-dimensioned if designed by considering the output results from the reference case (i.e., a model based on the axisymmetric hypothesis). Eventually, the accidental scenarios would not correspond to the reality.

4. Validation

Cronin and Evans [8] carried out a series of experiments to study the spreading of water within circular and squared bunds. The vessel, from which the water was released, represented a quadrant of a storage tank of 1.75 m of radius (see Fig. 16).

Table 4
Summary of post-processed data (maximum pool radius)

Case (#)	Description	Pool radius (m)	Distance from the tank wall (m)	Difference from the reference case (m)
1	Reference case	2.30	4.60	–
2	Radial spreading around a cylindrical tank	5.50	0.50	−4.10
3	Pool spreading around a parallelepiped tank	3.25	3.25	−1.35
4a	Pool spreading around a cylindrical tank (simplified case)	3.25	3.25	−1.35
4b	Pool spreading around a cylindrical tank (more rigorous case)	3.06	3.06	−1.54

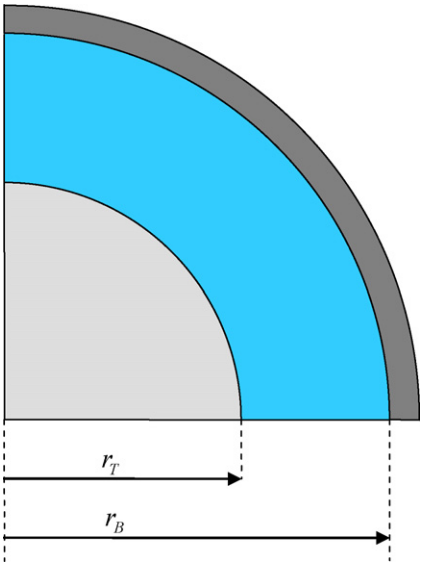

Fig. 16. Top view of the experimental apparatus used by Cronin and Evans [8].

The tank was filled with different amounts of water, from 3.5 to 4.3 m^3, at ambient temperature. The liquid release mechanism was put at the bottom of the tank, approximately at 2 cm from the ground, on the whole tank perimeter. The release mechanism allowed the water to flow from the tank onto a concrete pad. Sixty resistance probes drowned in the concrete bund floor monitored the movement of water.

The experiments from Cronin and Evans [8] involved three circular bund radii: 5, 7.1, and 10 m. In the first two cases, the spreading lasted less than 2 s, and our model for the simulation of axisymmetric spreading is not valid for spreading times lower than 1 s, as extensively reported in Webber and Jones [9]. Therefore, we validated our modeling approach only with the third set of data, related to water spreading into a bund of 10 m of radius. Five experiments were carried out, by varying the initial water height in the tank (1.449, 1.880, 1.808, 1.800, and 1.805 m).

We made a comparison between the conventional model (axisymmetric hypothesis) and our approach (pre- and post-processing of input an output data) looking at the simulation results of these models. As a common basis for the pool spreading, we used the model of Brambilla and Manca [10]. We assumed the area conservation hypothesis within the bund, which means that the available area is the same for both the experimental data and the corresponding simulation. Hence, the bund radius is the only value that must be pre-processed. From Eq. (2) we have

$$r_{B,axi} = \sqrt{r_B^2 - r_T^2} = \sqrt{(10)^2 - (1.75)^2} = 9.85\,m$$

Subsequently, we simulated the five experiments, characterized by a different initial water level inside the tank. Fig. 17 sketches the simulation setup based on the axisymmetric hypothesis. Aim of the simulations is determining the distance reached by the water from the tank wall.

Fig. 18 reports the comparison between the experimental data and the simulated results (not corrected data). The maximum distance reached by the axisymmetric pool is the axisymmetric bund diameter, i.e., 19.7 m (upper dashed line), while the maximum experimental distance is 8.25 m (lower dashed line). Each simulated line corresponds to a different initial condition (different liquid level inside the tank).

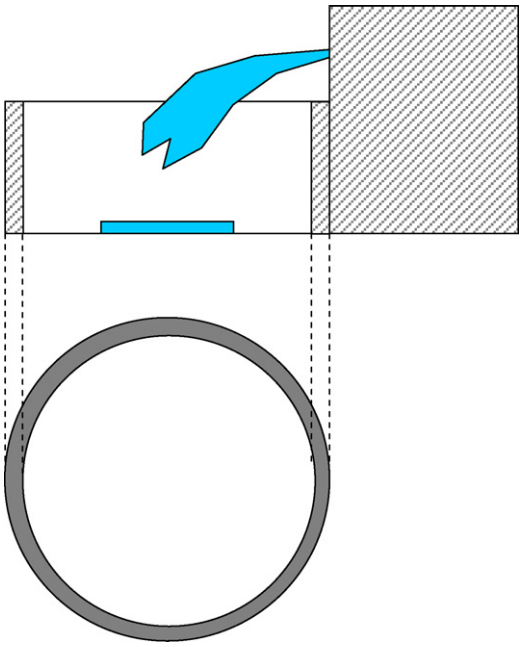

Fig. 17. Sketch of the axisymmetric simulation.

We performed also a simulation based on the pre- and post-processing of the input and output data. We chose the schematization discussed in Section 2.2. With reference to the input data, the radial velocity is evaluated as

$$u = u_e \frac{\sqrt{r_P^2 + r_T^2}}{r_P}$$

and it varies according to the liquid height in the tank.

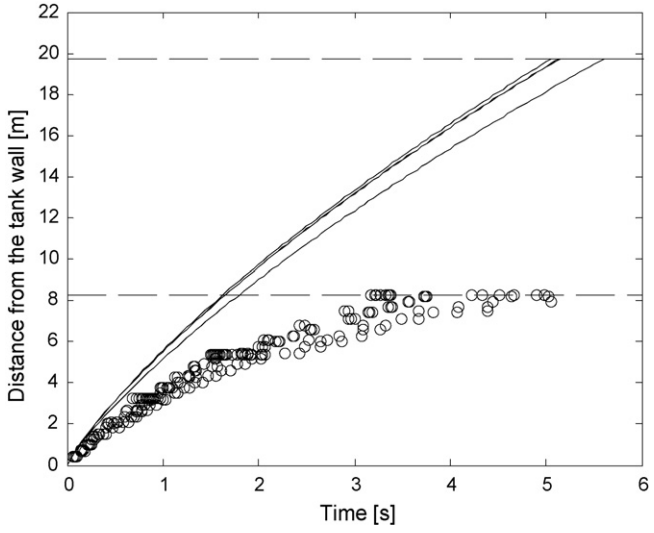

Fig. 18. Comparison between experimental data (circles) and simulated, not corrected, results (solid lines). The horizontal dashed lines quantify the maximum distance reached by the spreading liquid pools (lower experimental, higher simulated).

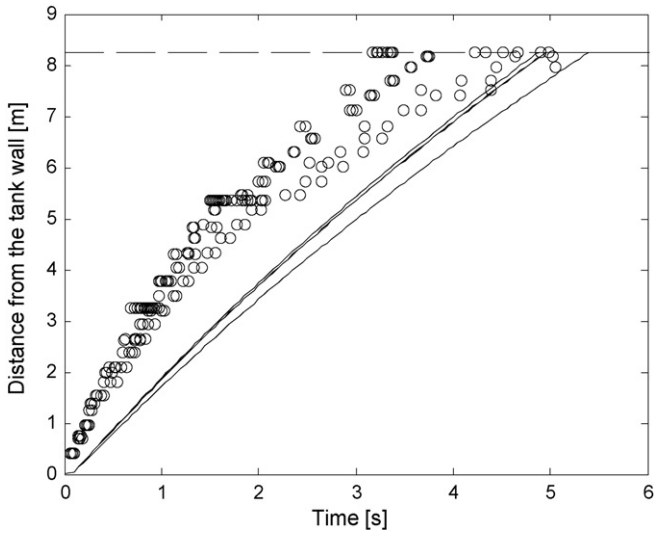

Fig. 19. Comparison between experimental data (circles) and simulated results (lines). The dashed line is the maximum distance reached by the spreading liquid.

As far as the output data are concerned, the corrected pool radii were modified according to Eq. (1).

Fig. 19 shows the comparison between the experimental data and the outcomes from the pre- and post-processing simulation model.

The corrected pool radii are in quite good agreement with the experimental data, especially for the time at which the water reaches the bund. Again, we want to remark that, below 1 s, the differences between the model and the experimental data are intrinsic of the model limitations.

According to this specific validation, we can conclude that the modeling approach proposed in this paper is consistent in reproducing the experimental data for the condition described in Section 2.2. It is worth observing that our modeling approach makes a little underestimation of pool radii respect to the experimental data. On the other hand, without pre- and post-processing the data, the overestimation of the maximum distance is too conservative (see the solid lines of Fig. 18). Therefore, our modeling approach may be used consistently for design purposes as well as for emergency planning.

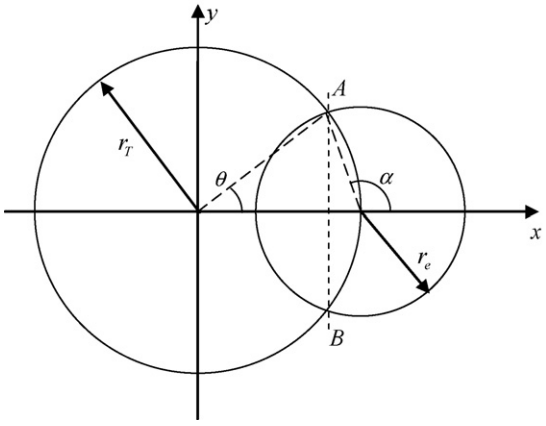

Fig. 20. Schematization of the pool-tank geometry.

We would like to emphasize that there is need for additional experimental data about the other conditions discussed in Section 2, to confirm the correctness of our modeling approach.

5. Conclusions

This paper made evident the importance of pre-processing the input data (to go from the real condition to the axisymmetric simulation) and post-processing the output results (to come back from the axisymmetric simulation to the real condition). In fact, under real conditions, the distances covered by the liquid can significantly differ from those evaluated by the reference case. This is of particular importance when designing mitigation systems or discussing accidental scenarios for emergency planning. If one chooses to confine the spreading of released liquids by building a bund around the possible epicenter, the design dimensions might be not proper for the real accident outcomes. Furthermore, a different arrangement of the mitigation systems, such as sprinklers, may be determined based on the modeling approach proposed in this paper.

The suggested approach is not a pure geometrical analysis. Conversely, it details a procedure for evaluating the most realistic pool attributes. We developed the simplified correlations instead of using a CFD code because CFD simulations are quite time consuming and cannot be applied when prompt accident simulations are needed either for emergency response or for operator training.

The comparisons between our modeling approach and experimental data show that they agree quite well, when applied to the second case-study (the only experimental data available in the literature). Further investigations are required to determine a similar agreement for the other case-studies.

Appendix A

In this section we give a detailed explanation on how to determine the corrected pool radius for the case-study 4b.

As mentioned before, the procedure for evaluating the corrected radius r_e is not explicit, but it is numerical and involves the evaluation of two definite integrals (see Fig. 20).

The bright-gray area of Fig. 13 can be evaluated as

$$A_1 = \int_{x_A}^{r_T} \sqrt{r_T^2 - x^2}\, dx$$

since

$$x = r_T \cos\phi, \qquad y = r_T \sin\phi$$

where ϕ is a generic angle between 0 and θ, this integral becomes:

$$A_1 = r_T^2(\theta - \sin\theta\cos\theta)$$

The dark-gray plus the bright-gray areas of Fig. 13 can be evaluated as

$$A_1 + A_2 = \int_{x_A}^{r_T+r_e} \sqrt{2r_T x - x^2 + r_e^2 - r_T^2}\, dx$$

since

$$x = r_T + r_e \cos\phi, \qquad y = r_e \sin\phi$$

where ϕ is a generic angle between 0 and α, this integral becomes:

$$A_1 + A_2 = r_e^2(\alpha - \sin\alpha\cos\alpha)$$

The angles α and θ can be found from the trigonometric relations referred to the intersection points:

$$x_A = \frac{2r_T^2 - r_e^2}{2r_T} = r_T\cos\theta = r_T + r_e\cos\alpha,$$

$$y_A = r_e\sqrt{1 - \frac{r_e^2}{4r_T^2}} = r_T\sin\theta = r_e\sin\alpha$$

Finally, the dark-gray portion of Fig. 13 can be evaluated as

$$A_2 = (A_1 + A_2) - A_1 = r_e^2(\alpha - \sin\alpha\cos\alpha) - r_T^2(\theta - \sin\theta\cos\theta)$$

References

[1] J.A. Fay, The spread of oil slick on calm sea, in: D.P. Hoult (Ed.), Oil on the Sea, Plenum Press, New York, 1969.

[2] D.P. Hoult, Oil spreading on the sea, Annu. Rev. Fluid Mech. 4 (1972) 341–368.

[3] H.R. Chang, R.C. Reid, J.A. Fay, Boiling and spreading of liquid nitrogen and liquid methane on water, Int. Comm. Heat Mass Transfer 10 (1983) 253–263.

[4] D.M. Webber, P.W.M. Brighton, Inviscid similarity solutions for slumping from a cylindrical tank, Trans. ASME 108 (1986) 238–240.

[5] D.M. Webber, A model for pool spreading and vaporization and its implementation in the computer code G*A*S*P, SRD/HSE/R507, AEA Technology, 1990.

[6] H.W.M. Witlox, Model for pool spreading, evaporation and solution on land and water (PVAP)—theory manual, Consequence modeling documentation (PHAST Technical Reference), 2000.

[7] C.J.H. Van der Bosch, Pool evaporation, in: C.J.H. Van der Bosch, R.A.M.P. Weterings (Eds.), Methods for the Calculation of Physical Effects due to Releases of Hazardous Materials (Liquids and Gases) ("Yellow book"), TNO, The Hague, Netherlands, 2005.

[8] P.S. Cronin, J.A. Evans, A series of experiments to study the spreading of liquid pools with different bund arrangements, HSE Contract Research Report 405/2002, Advantica Technologies Limited, 2002.

[9] D.M. Webber, S.J. Jones, A model of spreading vaporising pools, in: Woodward (Ed.), International Conference on Vapor Cloud Modelling, AIChE, Boston, MA, USA, 1987.

[10] S. Brambilla, D. Manca, Accidents involving liquids: a step ahead in modeling pool spreading, evaporation and burning, J. Hazard. Mater., submitted for publication.